ACS Macro Letters

pubs.acs.org/macroletters Letter

Spiral Hierarchical Superstructures from Twisted Ribbons of Self-Assembled Chiral Block Copolymers

Kai-Chieh Yang and Rong-Ming Ho*

Cite This: ACS Macro Lett. 2020, 9, 1130−1134 Read Online

ACCESS | Metrics & More | Article Recommendations | Supporting Information

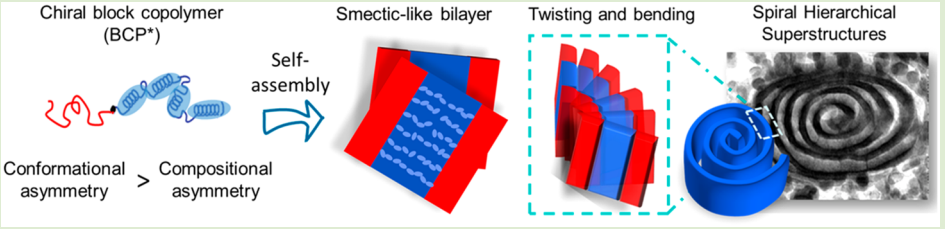

ABSTRACT: Spiral hierarchical superstructures were found in the self-assembly of chiral block copolymers (BCPs*) composed of a chiral poly(L-lactide) (PLLA) and an achiral polystyrene (PS) as major and minor blocks, respectively. The PLLA helical chain with semiflexible rod-like character as compared to the random coil of PS results in self-assembly with a conformational asymmetry effect overwhelming the compositional one. Consequently, instead of the forming PS cylinder microdomains in the PLLA matrix, a smectic liquid-crystal-like bilayer sandwiched with PLLA and PS microdomains will be formed. Owing to twisting and bending due to the chiral cholesteric liquid-crystal-like force field combined with steric hindrance at the chiral interface, the forming bilayers (twisted ribbon) will develop into either a concentric lamellar texture from scrolling or roll-cake textures from spiraling. This study might bring a concept for the formation of spiral hierarchical superstructures from self-assembled bilayers for device application.

Downloaded via SYNCHROTRON RADIATION RESEARCH on January 27, 2021 at 03:01:29 (UTC).
See https://pubs.acs.org/sharingguidelines for options on how to legitimately share published articles.

Concentric and spiral multilayered nanostructures are considered as important geometries for signal enhancement of devices,[1,2] optical metamaterials,[3−5] plasmonics,[6−8] and photonics.[9,10] For structure fabrication in nanometer length scale with tunable microdomain size, the self-assembly of block copolymers (BCPs) which gives various ordered morphologies through microphase separation is suggested as a facile approach. Conventional phases such as sphere, cylinder, gyroid, and lamellae can be formed sequentially with the increase of minor block volume fraction in the self-assembly of coil−coil BCPs,[11,12] and a symmetric phase diagram can be found for the BCPs with composition asymmetry in constituted blocks.[13,14] Nevertheless, concentric rings are not commonly formed from BCP self-assembly except under specific self-assembling environments such as confined self-assembly,[15−18] while spiral morphologies have not been found.

A block copolymer composed of a chiral segment is denoted as a chiral block copolymer (BCP*).[19−21] A series of chiral diblock copolymers, polystyrene-*block*-poly(L-lactide) (PS−PLLA) composed of major achiral PS and minor chiral PLLA blocks (referred to as PS-rich PS−PLLA BCPs*), has been synthesized for self-assembly; a helical phase (H*), PLLA multichain helical cylinders microdomain hexagonally packed in the PS matrix, can be found.[20,21] A helical conformation of the chiral polylactides with preferred helicity can be formed due to intrachain chiral interactions, as evidenced by vibrational circular dichroism (VCD) results.[22−24] The persistence length of the chiral polylactide with helical conformation is indeed larger than the achiral polystyrene block with random coil character,[20] giving a semiflexible rod−coil diblock copolymer system with conformational asymmetry.[25−28] The formation of the H* in the self-assembled PS−PLLA is attributed to the formation of the PLLA cylinder microdomain in the PS matrix due to compositional asymmetry combined with the twisting and shifting of the cylinder resulting from interchain chiral interactions.[22,29,30] In this study, we aim to systematically examine the mutual interactions of the conformational and compositional asymmetry effects on the phase behaviors of BCPs*. In contrast to the PS-rich PS−PLLA BCPs*, the effects of conformational and compositional asymmetry on the self-assembled phase behaviors of PLLA-rich PS−PLLA with major chiral PLLA (semiflexible rod) and minor achiral PS (random coil) blocks will be intuitively different. Spiral hierarchical superstructures from twisted ribbons instead of helical cylinders can be formed in the PLLA-rich PS−PLLA BCPs*, giving rise to the formation of concentric lamellar and roll-cake superstructures in the bulk that sheds the light to create hierarchical

Received: June 1, 2020
Accepted: July 21, 2020
Published: July 22, 2020

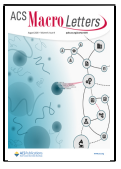

ACS Publications © 2020 American Chemical Society

https://dx.doi.org/10.1021/acsmacrolett.0c00415
ACS Macro Lett. 2020, 9, 1130−1134

superstructures with concentric and spiral rings simply from self-assembly.

As shown in Figure 1a, the small-angle X-ray scattering (SAXS) result of the solution-cast sample gives broadened

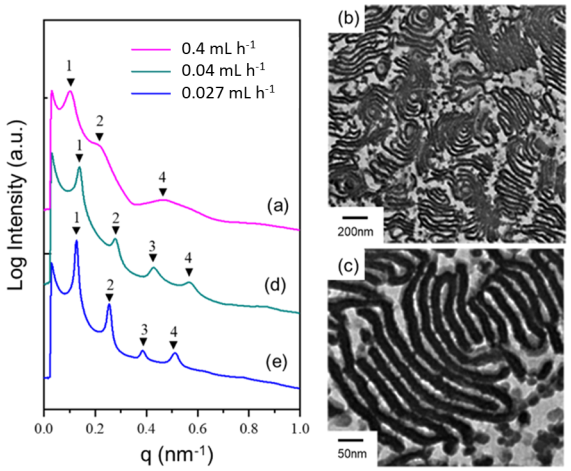

Figure 1. 1D SAXS profiles of self-assembled PS24−PLLA67 from solution casting with a solvent evaporation rate of (a) 0.4 mL h^{-1}, (d) 0.04 mL h^{-1}, and (e) 0.027 mL h^{-1}. (b) Corresponding TEM micrograph of part a. (c) Enlarged micrograph of tortuous lamellae in part b.

reflections at the relative q values of 1:2:4, suggesting the formation of a typical lamellar phase for the self-assembled PS−PLLA ($M_{n,PS}$ = 24,100 g mol^{-1}; $M_{n,PLLA}$ = 66,900 g mol^{-1}; $Đ$ = 1.30; f_{PLLA}^{v} = 0.70, denoted as PS24−PLLA67; see the Supporting Information for details including GPC, NMR, and thermal properties analysis). To further examine the self-assembled hierarchical superstructures, transmission electron microscopy (TEM) experiments were carried out. As shown in Figure 1b, instead of parallel lamellar projection, there is a tortuous lamellar texture in the bright matrix at which the PS microdomains appear dark due to RuO_4 staining and the bright regions are PLLA microdomains. The enlarged image of the tortuous lamellar texture (Figure 1c) suggests the formation of multilayered lamellae, resulting from a bilayer ribbon sandwiched with PS and PLLA multichain microdomains. With the reduction of the solvent evaporation rate for solution casting to 0.04 mL h^{-1}, significant variations on the self-assembled morphologies can be observed. In contrast to Figure 1c, two distinctive projections with concentric ring (Figure 2a)

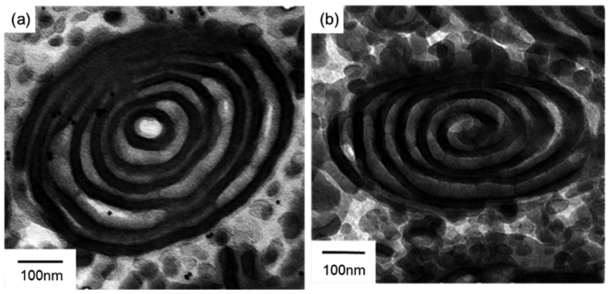

Figure 2. TEM micrographs of self-assembled PS24−PLLA67 from solution casting with a solvent evaporation rate of 0.04 mL h^{-1}: (a) concentric lamellar and (b) roll-cake textures from curved multilayered lamellae.

and roll-cake textures (Figure 2b) can be found, inferring the formation of curved multilayered lamellae from the bilayer ribbons. As shown in Figure S10, morphologies with different textures including curved multilayered lamellae and disordered ones can be clearly identified from the low magnification TEM image. Corresponding SAXS results further confirm the formation of suggested multilayered lamellae at which sharpening of the reflection peaks at the relative q values of 1:2:3:4 can be clearly identified (Figure 1d); based on the primary reflection in the SAXS profile, the calculated interdomain distance (i.e., d-spacing) is approximately 45 nm as compared to the one with 61 nm from fast casting (Figure 1a). Note that WAXD results of the self-assembled samples (Figure S11) suggest no crystallization effects on the forming phase with different solvent evaporation rates.[31,32]

To further examine the morphologies of the curved multilayered lamellae in the form of bilayer ribbons, SEM observations were carried out on hydrolyzed samples at which the PLLA can be degenerated by hydrolysis in NaOH aqueous solution to leave the textures of the PS for imaging. As shown in Figure 3, curved sheet-like textures could be clearly

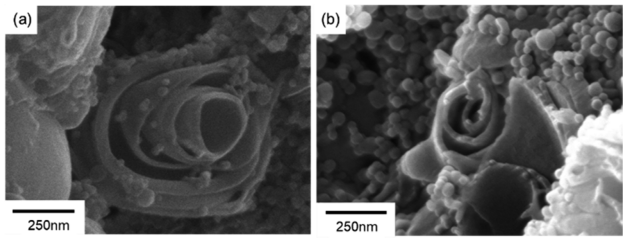

Figure 3. FESEM micrographs of hydrolyzed PS24−PLLA67 from solution casting with a solution evaporation rate of 0.04 mL h^{-1}: (a) concentric columnar-like texture and (b) rolling lamellar texture in a spiral fashion of the PS microdomains after removal of the PLLA.

identified at which the curving might scroll up the bilayer ribbons to give columnar-like PS microdomains with concentric texture from scrolliing (Figure 3a) or develop in a spiral fashion to form rolling lamellar textures from spiraling (Figure 3b). Also, visualization of the PLLA microdomains was conducted by templated sol−gel reaction using hydrolyzed PS−PLLA as templates followed by removal of the PS through UV exposure.[33] Similar to the imaging results in Figure 3, the PLLA microdomain is indeed a curved lamellar with sheet-like texture resembling the one from the PS at which the PLLA microdomains can be faithfully preserved after SiO_2 replication (Figure S12). Consequently, based on the TEM and SEM observations, the self-assembled PS−PLLA is indeed a bilayer type to give the formation of curved mulilayered lamellae.

Interestingly, those concentric lamellar and roll-cake textures were surrounded by disordered textures, resulting from solution casting through fast evaporation; the corresponding phase behaviors are different from the formation of conventional ordered phases directly from microphase separation, implicitly implying that the formation of the unique hierarchical superstructures is kinetically controlled through morphological evolution of the curved mulilayered lamellae from the nucleation and growth process of microphase separation. Note that the nucleation and growth process was initiated from solution casting with gradual removal of the solvent. To examine the suggested mechanism of the forming phases through the kinetically controlled process, a solution-

https://dx.doi.org/10.1021/acsmacrolett.0c00415
ACS Macro Lett. 2020, 9, 1130−1134

cast sample was acquired by lowering the solvent evaporation rate at 0.027 mL h^{-1}. After the decrease of solvent evaporation rate, the monograin sizes of the concentric lamellar (Figure 4a)

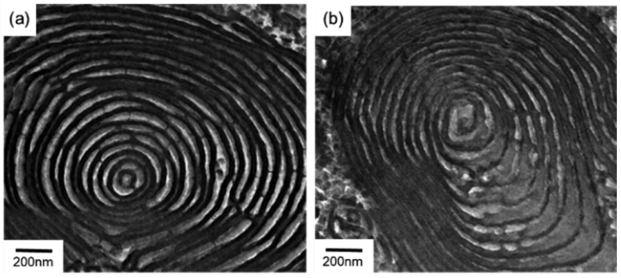

Figure 4. TEM micrographs of self-assembled PS24−PLLA67 from solution casting with a solvent evaporation rate of 0.027 mL h^{-1}: (a) concentric lamellar and (b) roll-cake textures from curved multilayered lamellae.

and roll-cake textures (Figure 4b) can be significantly increased, as evidenced by the intensified reflection peaks at the relative q values of 1:2:3:4 (Figure 1e). On the basis of Scherrer equation analysis, the ordering domain size can be increased by reducing the evaporation rate. The growth of the ordering domain size can be increased to approximately 1100 nm from 550 nm for the one with faster evaporation; the scattering results are in line with the TEM observation. With further reducing the evaporation rate at 0.0008 mL h^{-1}, the growth of the curved mulilayered lamellae leads to the formation of undulated lamellae without disorder regions (Figure S13a); the corresponding SAXS result (Figure S13b) gives reflection peaks at the relative q values of 1:2:3:4:5:6:7.

The self-assembling behaviors of the PLLA-rich PS−PLLAs, in comparison with the ones with PS-rich PS−PLLA, were generalized by synthesizing samples with equivalent volume fraction but different molecular weights (PS10−PLLA24 and PS17−PLLA42 besides PS24−PLLA67), as listed in Table S1 (see the Supporting Information for a detailed discussion including GPC, NMR, and thermal properties analysis), at which similar results from imaging (Figure S14) and scattering (Figure S15) suggest the generic formation of a curved multilayered lamellar phase in the PLLA-rich PS−PLLAs. Note that, at equivalent asymmetry in composition for the ones with the minor block from volume fraction 0.3 to 0.4, there is an obvious difference between the self-assembled PS-rich and PLLA-rich PS−PLLAs; the PS-rich ones give the formation of a helical cylinder in the H*, whereas the PLLA-rich ones form the curved mulilayered lamellae to give the concentric lamellar and roll-cake textures different to conventional textures predicted from coil−coil block copolymer self-assembly. Namely, there should be a unique progression of self-assembled morphologies such as the situation in transitioning from the case of coil−coil[11,12] to rod−coil[34−37] copolymers.

As illustrated in Figure 5a, starting with the helical PLLA chain that gives a longer persistence length (1.19 nm)[20] than the PS coil (0.92 nm),[38] giving the PLLA with semiflexible rod character due to the helical conformation, the conformational asymmetry between the PS and PLLA blocks gives the conformational asymmetry effect[14] overwhelming the compositional one[26,27] on microphase separation for the formation of bilayer microdomains instead of PS cylinder microdomains in the PLLA matrix once the semiflexible rod is a major block in the diblock copolymer. Consequently, as illustrated in Figure

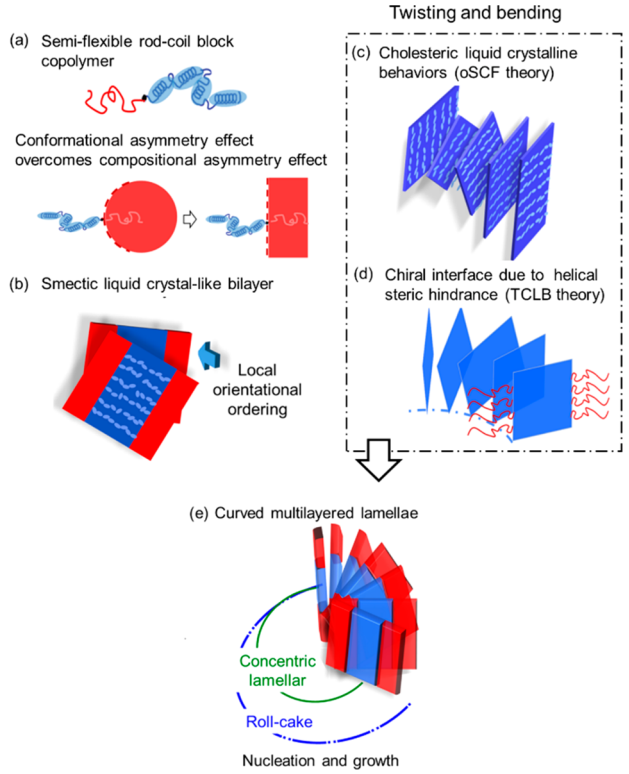

Figure 5. Schematic illustration for the semiflexible rod−coil block copolymer with a helical chain as the major block (a), resulting in a smectic liquid-crystal-like bilayer (b), followed by twisting and bending due to the chiral cholesteric liquid-crystal-like force field (c) combined with steric hindrance at the chiral interface (d) to scroll the twisted ribbon into a concentric texture or develop in a spiral fashion to form a roll-cake texture (e) through a nucleation and growth mechanism for microphase separation.

5b, the self-assembly of the semiflexible PLLA chains gives rise to the formation of liquid-crystalline texture that results in the smectic liquid-crystal-like bilayer packing with frustration instead of a cylindrical one from the consideration of the compositional asymmetry effect. Accordingly, the morphologies in the semiflexible-rod-block (PLLA)-rich region of the phase diagram of PS−PLLA should be intrinsically asymmetric to the one with the coil-block-rich region. As found, the transformation from the cylinder to lamellar phases with increasing persistence length can be recognized and rationalized as a consequence of forming orientational ordering and resultant packing frustration of those semirigid PLLA chains. With the twisting of the smectic liquid-crystal-like bilayer texture due to the cholesteric liquid-crystalline behaviors with chirality effects as proposed by Grason (orientational self-consistent field (oSCF) theory)[39,40] (Figure 5c) and the bending of the bilayer texture initiating from the chiral interface due to helical steric hindrance as proposed by Ou-Yang (tilted chiral lipid bilayer (TCLB) theory)[41,42] (Figure 5d), it is expected to lead the formation of hierarchical superstructures from twisted ribbon (Figure 5e) to develop as the concentric lamellar texture from scrolling and roll-cake texture from spiraling. To examine the suggested packing of cholesteric liquid-crystal-like texture with helical sense, vibrational circular dichroism (VCD) experiments were carried out. As shown in Figure S16, in contrast to the null signal in dilute solution, a VCD signal with split-type Cotton effect in the wavenumber range from 1300 to 1100 cm^{-1}, corresponding to

https://dx.doi.org/10.1021/acsmacrolett.0c00415
ACS Macro Lett. 2020, 9, 1130−1134

the absorption of the C−O−C vibrational mode, can be clearly identified in the solid state. As the C−O−C vibration mode is parallel to the main chain, it thus suggests that the VCD signal is originated from the twisting of helical PLLA chains due to interchain chiral interactions for packing with orientational order.[24] Notably, the VLD results in Figure S17 show that the effect of anisotropic character is insignificant.

In conclusion, a new morphology, curved multilayered lamellae with concentric lamellar and roll-cake textures from scrolling or spiraling of twisted ribbon, was found in the self-assembly of PLLA-rich PS−PLLA through control of morphological evolution from the kinetic control of the nucleation and growth of microphase separation. In contrast to the forming helical cylinder in PS-rich PS−PLLA, the formation of a twisted ribbon with sheet-like texture in the PLLA-rich PS−PLLA reveals the relief of the compositional asymmetry effect on self-assembly by the conformational asymmetry effect due to the chiral block with longer persistence length. Namely, a block copolymer which contains a semiflexible rod block as a major block fortifies the liquid-crystal behavior for self-assembly of the block copolymer, giving the formation of a smectic liquid-crystal-like bilayer. The chirality effects on BCP self-assembly give rise to the twisting and bending of the bilayer initiated by the chiral cholesteric liquid-crystal-like force field combined with steric hindrance at the chiral interface, resulting in the formation of a spiral hierarchical superstructure. The forming geometries with spiral character are appealing in the applications of a wide range such as signal enhancement of devices, optical metamaterials, plasmonics, and photonics.

■ ASSOCIATED CONTENT

Supporting Information

The Supporting Information is available free of charge at https://pubs.acs.org/doi/10.1021/acsmacrolett.0c00415.

Additional information, table, and figures related to materials preparation, thermal properties, low magnification TEM image for curved multilayered lamellae, examination of crystallization effects on self-assembled hierarchical superstructures, templated sol−gel reaction of multilayered lamellar structure, morphological evolution of PLLA-rich PS−PLLA from self-assembly, PLLA-rich PS−PLLA samples with equivalent volume fraction but different molecular weights, evidence for interchain chiral interactions of self-assembled PLLA-rich PS−PLLA, and anisotropic effect on the VCD spectrum (PDF)

■ AUTHOR INFORMATION

Corresponding Author

Rong-Ming Ho − *Department of Chemical Engineering, National Tsing Hua University, Hsinchu 30013, Taiwan;* orcid.org/0000-0002-2429-7617; Email: rmho@mx.nthu.edu.tw

Author

Kai-Chieh Yang − *Department of Chemical Engineering, National Tsing Hua University, Hsinchu 30013, Taiwan*

Complete contact information is available at: https://pubs.acs.org/10.1021/acsmacrolett.0c00415

Notes

The authors declare no competing financial interest.

■ ACKNOWLEDGMENTS

The National Synchrotron Radiation Research Center (NSRRC) for its assistance in the Synchrotron SAXS experiments. This work is supported in part by the Ministry of Education, Taiwan, R.O.C., under the Higher Education Sprout Project.

■ REFERENCES

(1) Chen, W.; Abeysinghe, D. C.; Nelson, R. L.; Zhan, Q. Plasmonic Lens Made of Multiple Concentric Metallic Rings under Radially Polarized Illumination. *Nano Lett.* **2009**, *9*, 4320.

(2) Zeng, J.; Gao, J.; Luk, T. S.; Litchinitser, N. M.; Yang, X. Structuring Light by Concentric-Ring Patterned Magnetic Metamaterial Cavities. *Nano Lett.* **2015**, *15*, 5363.

(3) Pendry, J. B. A Chiral Route to Negative Refraction. *Science* **2004**, *306*, 1353.

(4) Liu, Z.; Lee, H.; Xiong, Y.; Sun, C.; Zhang, X. Far-Field Optical Hyperlens Magnifying Sub-Diffraction-Limited Objects. *Science* **2007**, *315*, 1686.

(5) Kan, T.; Isozaki, A.; Kanda, N.; Nemoto, N.; Konishi, K.; Takahashi, H.; Kuwata-Gonokami, M.; Matsumoto, K.; Shimoyama, I. Enantiomeric Switching of Chiral Metamaterial for Terahertz Polarization Modulation Employing Vertically Deformable MEMS Spirals. *Nat. Commun.* **2015**, *6*, 8422.

(6) Radloff, C.; Halas, N. J. Plasmonic Properties of Concentric Nanoshells. *Nano Lett.* **2004**, *4*, 1323.

(7) Trevino, J.; Cao, H.; Dal Negro, L. Circularly Symmetric Light Scattering from Nanoplasmonic Spirals. *Nano Lett.* **2011**, *11*, 2008.

(8) Cho, S.-Y.; Jeon, H.-J.; Yoo, H.-W.; Cho, K. M.; Jung, W.-B.; Kim, J.-S.; Jung, H.-T. Highly Enhanced Fluorescence Signals of Quantum Dot−Polymer Composite Arrays Formed by Hybridization of Ultrathin Plasmonic Au Nanowalls. *Nano Lett.* **2015**, *15*, 7273.

(9) Vekris, E.; Ozin, G. A.; Kitaev, V. Curling Colloidal Photonic Crystals. *Adv. Mater.* **2006**, *18*, 2481.

(10) Kolle, M.; Lethbridge, A.; Kreysing, M.; Baumberg, J. J.; Aizenberg, J.; Vukusic, P. Bio-Inspired Band-Gap Tunable Elastic Optical Multilayer Fibers. *Adv. Mater.* **2013**, *25*, 2239.

(11) Bates, F. S.; Fredrickson, G. H. Block Copolymer Thermodynamics: Theory and Experiment. *Annu. Rev. Phys. Chem.* **1990**, *41*, 525.

(12) Bates, F. S.; Fredrickson, G. H. Block Copolymers—Designer Soft Materials. *Phys. Today* **1999**, *52*, 32.

(13) Khandpur, A. K.; Foerster, S.; Bates, F. S.; Hamley, I. W.; Ryan, A. J.; Bras, W.; Almdal, K.; Mortensen, K. Polyisoprene-Polystyrene Diblock Copolymer Phase Diagram near the Order-Disorder Transition. *Macromolecules* **1995**, *28*, 8796.

(14) Matsen, M. W.; Bates, F. S. Unifying Weak- and Strong-Segregation Block Copolymer Theories. *Macromolecules* **1996**, *29*, 1091.

(15) Shin, K.; Xiang, H.; Moon, S. I.; Kim, T.; McCarthy, T. J.; Russell, T. P. Curving and Frustrating Flatland. *Science* **2004**, *306*, 76.

(16) Li, L.; Matsunaga, K.; Zhu, J.; Higuchi, T.; Yabu, H.; Shimomura, M.; Jinnai, H.; Hayward, R. C.; Russell, T. P. Solvent-Driven Evolution of Block Copolymer Morphology under 3D Confinement. *Macromolecules* **2010**, *43*, 7807.

(17) Ma, M.; Titievsky, K.; Thomas, E. L.; Rutledge, G. C. Continuous Concentric Lamellar Block Copolymer Nanofibers with Long Range Order. *Nano Lett.* **2009**, *9*, 1678.

(18) Kim, S. H.; Weitz, D. A. One-step Emulsification of Multiple Concentric Shells with Capillary Microfluidic Devices. *Angew. Chem., Int. Ed.* **2011**, *50*, 8731.

(19) Ho, R.-M.; Chiang, Y.-W.; Tsai, C.-C.; Lin, C.-C.; Ko, B.-T.; Huang, B.-H. Three-Dimensionally Packed Nanohelical Phase in Chiral Block Copolymers. *J. Am. Chem. Soc.* **2004**, *126*, 2704.

(20) Ho, R.-M.; Chiang, Y.-W.; Chen, C.-K.; Wang, H.-W.; Hasegawa, H.; Akasaka, S.; Thomas, E. L.; Burger, C.; Hsiao, B. S. Block Copolymers with a Twist. *J. Am. Chem. Soc.* **2009**, *131*, 18533.
(21) Ho, R.-M.; Chiang, Y.-W.; Lin, S.-C.; Chen, C.-K. Helical Architectures from Self-assembly of Chiral Polymers and Block Copolymers. *Prog. Polym. Sci.* **2011**, *36*, 376.
(22) Ho, R.-M.; Li, M.-C.; Lin, S.-C.; Wang, H.-F.; Lee, Y.-D.; Hasegawa, H.; Thomas, E. L. Transfer of Chirality from Molecule to Phase in Self-Assembled Chiral Block Copolymers. *J. Am. Chem. Soc.* **2012**, *134*, 10974.
(23) Wen, T.; Wang, H.-F.; Li, M.-C.; Ho, R.-M. Homochiral Evolution in Self-Assembled Chiral Polymers and Block Copolymers. *Acc. Chem. Res.* **2017**, *50*, 1011.
(24) Wang, H.-F.; Yang, K.-C.; Hsu, W.-C.; Lee, J.-Y.; Hsu, J.-T.; Grason, G. M.; Thomas, E. L.; Tsai, J.-C.; Ho, R.-M. Generalizing the Effects of Chirality on Block Copolymer Assembly. *Proc. Natl. Acad. Sci. U. S. A.* **2019**, *116*, 4080.
(25) Joziasse, C. A. P.; Veenstra, H.; Grijpma, D. W.; Pennings, A. J. On the Chain Stiffness of Poly(lactide)s. *Macromol. Chem. Phys.* **1996**, *197*, 2219.
(26) Bates, F. S.; Fredrickson, G. H. Conformational Asymmetry and Polymer-Polymer Thermodynamics. *Macromolecules* **1994**, *27*, 1065.
(27) Bates, F. S.; Schulz, M. F.; Khandpur, A. K.; Förster, S.; Rosedale, J. H.; Almdal, K.; Mortensen, K. Fluctuations, Conformational Asymmetry and Block Copolymer Phase Behaviour. *Faraday Discuss.* **1994**, *98*, 7.
(28) Yu, B.; Danielsen, S. P. O.; Patterson, A. L.; Davidson, E. C.; Segalman, R. A. Effects of Helical Chain Shape on Lamellae-Forming Block Copolymer Self-Assembly. *Macromolecules* **2019**, *52*, 2560.
(29) Li, M.-C.; Wang, H.-F.; Chiang, C.-H.; Lee, Y.-D.; Ho, R.-M. Lamellar-Twisting-Induced Circular Dichroism of Chromophore Moieties in Banded Spherulites with Evolution of Homochirality. *Angew. Chem., Int. Ed.* **2014**, *53*, 4450.
(30) Wen, T.; Ho, R.-M. Effects of the Chiral Interface and Orientation-Dependent Segmental Interactions on Twisting of Self-Assembled Block Copolymers. *ACS Macro Lett.* **2017**, *6*, 370.
(31) Chiang, Y.-W.; Ho, R.-M.; Thomas, E. L.; Burger, C.; Hsiao, B. S. A Spring-Like Behavior of Chiral Block Copolymer with Helical Nanostructure Driven by Crystallization. *Adv. Funct. Mater.* **2009**, *19*, 448.
(32) Chen, C.-K.; Lin, S.-C.; Ho, R.-M.; Chiang, Y.-W.; Lotz, B. Kinetically Controlled Self-Assembled Superstructures from Semicrystalline Chiral Block Copolymers. *Macromolecules* **2010**, *43*, 7752.
(33) Tseng, W.-H.; Chen, C.-K.; Chiang, Y.-W.; Ho, R.-M.; Akasaka, S.; Hasegawa, H. Helical Nanocomposites from Chiral Block Copolymer Templates. *J. Am. Chem. Soc.* **2009**, *131*, 1356.
(34) Chen, J. T.; Thomas, E. L.; Ober, C. K.; Hwang, S. S. Zigzag Morphology of a Poly(styrene-6-hexyl isocyanate) Rod-Coil Block Copolymer. *Macromolecules* **1995**, *28*, 1688.
(35) Chen, J. T.; Thomas, E. L.; Ober, C. K.; Mao, G.-P. Self-Assembled Smectic Phases in Rod-Coil Block Copolymers. *Science* **1996**, *273*, 343.
(36) Olsen, B. D.; Segalman, R. A. Structure and Thermodynamics of Weakly Segregated Rod−Coil Block Copolymers. *Macromolecules* **2005**, *38*, 10127.
(37) Olsen, B. D.; Segalman, R. A. Nonlamellar Phases in Asymmetric Rod−Coil Block Copolymers at Increased Segregation Strengths. *Macromolecules* **2007**, *40*, 6922.
(38) Brûlet, A.; Boué, F.; Cotton, J. About the Experimental Determination of the Persistence Length of Wormlike Chains of Polystyrene. *J. Phys. II* **1996**, *6*, 885.
(39) Zhao, W.; Russell, T. P.; Grason, G. M. Chirality in Block Copolymer Melts: Mesoscopic Helicity from Intersegment Twist. *Phys. Rev. Lett.* **2013**, *110*, No. 058301.
(40) Grason, G. M. Chirality Transfer in Block Copolymer Melts: Emerging Concepts. *ACS Macro Lett.* **2015**, *4*, 526.
(41) Ou-Yang, Z.-c.; Liu, J.-x. Helical Structures of Tilted Chiral Lipid Bilayers Viewed as Cholesteric Liquid Crystals. *Phys. Rev. Lett.* **1990**, *65*, 1679.
(42) Ou-Yang, Z.-c.; Liu, J. Theory of Helical Structures of Tilted Chiral Lipid Bilayers. *Phys. Rev. A: At., Mol., Opt. Phys.* **1991**, *43*, 6826.

https://dx.doi.org/10.1021/acsmacrolett.0c00415
ACS Macro Lett. 2020, 9, 1130−1134